Nonadiabatic Trajectories at an Exhibition

2 **AUTHORS**, INCLUDING:

Donald Truhlar

University of Minnesota Twin Cities

1,342 PUBLICATIONS   **81,524** CITATIONS

SEE PROFILE

FEATURE ARTICLE

Nonadiabatic Trajectories at an Exhibition

Michael D. Hack and Donald G. Truhlar*

Department of Chemistry and Supercomputer Institute, University of Minnesota, Minneapolis, Minnesota 55455-0431

Received: April 27, 2000; In Final Form: June 13, 2000

The present article reviews two classes of semiclassical (mixed quantum mechanical/classical) methods for investigating multielectronic-state dynamics: the trajectory surface-hopping (TSH) method and the time-dependent self-consistent field (TDSCF) method. The recent availability of accurate quantum mechanical dynamics calculations for a variety of realistic three-body two-state potential energy matrices has allowed an assessment of the validity of semiclassical multisurface dynamics methods that are applicable to larger systems. These studies indicate that Tully's fewest switches algorithm is the best available TSH method and that the Ehrenfest method is the best previously available TDSCF method. The fewest switches surface-hopping method has relatively small errors even when it is not the best method while the Ehrenfest TDSCF method tends to have larger errors when it is not the best. However, the fewest switches algorithm involves unphysical discontinuities in momenta, and the results may depend on the choice of representation. Furthermore, the surface-hopping algorithm is frequently frustrated in its attempt to maintain ensemble-average self-consistency. The Ehrenfest method removes all these troublesome aspects but at the cost of producing unphysical mixed states, which are responsible for its larger errors in observables. A recently introduced TDSCF method, the continuous surface-switching method, removes the unphysical mixed states of the Ehrenfest method, and in initial tests it produces results that are systematically better than those calculated by the Ehrenfest method. The present article illustrates several of these aspects of nonadiabatic trajectory methods pictorially.

I. Introduction

Semiclassical dynamical methods, that is, dynamical theories that combine classical mechanics and quantum mechanics,[1,2] provide an appealing way to gain insight into systems for which accurate quantum mechanical calculations are intractable or in which a better understanding of experimental results is desired. Purely classical dynamical methods[3,4] (or quasiclassical methods,[5,6] which are classical trajectories with quantized initial conditions) are often applied to systems that are too large to study quantum mechanically; however, in many cases multiple electronic states are involved, and some method beyond the Born—Oppenheimer approximation must be employed for treating the inherently quantum mechanical electronic degrees

of freedom.[7,8] It is still the case that for systems with more than three atoms and more than one electronic state a converged quantum mechanical description is infeasible; in fact, only recently have accurate descriptions of full three-dimensional three-body two-electronic-state systems been presented.[9-27] Nevertheless, there is a strong interest in large photochemical systems,[28-31] and there is a corresponding interest in the development of accurate semiclassical methods that might be applicable to such problems.

Until recently, the lack of benchmark accurate quantal results has prevented a validation of the various semiclassical methods that have been proposed. In our view, systematic testing of existing methods is the first step toward understanding their

strengths and weaknesses and, we hope, toward developing improved methods. This report summarizes our recent work on testing different kinds of semiclassical methods on a variety of electronically nonadiabatic chemical reaction types in gas-phase systems. We hope to understand which semiclassical methods can provide a useful description of the dynamics for various cases so that we or others can use this information to design improved methods that will be accurate for a wide range of systems. In this paper we review our recent work and try to determine which, if any, of the semiclassical methods we have examined thus far is the best and for which systems each of the methods we consider is likely to be accurate.

The work presented here should be of interest to a broad cross section of chemists, and since these groups often use quite different words to describe the same phenomena and similar concepts, a few words on nomenclature and background should be helpful. All chemical processes may be divided into two classes: those in which the electronic state does not change and those in which it does. For nonreactive collisions these may be called *electronically elastic* and *electronically inelastic*, respectively. A very similar but somewhat less precise distinction is implied by the common terms *thermal reactions*[28-31] for reactions initiating in the ground electronic state, *photochemical reactions*[28-31] for those initiating in an electronically excited state, and, less frequently encountered, *chemiluminescent reactions* for those producing an electronically excited species. At a more detailed level of understanding, one categorizes a process not just on the basis of initial and final states, but on the evolution of these states throughout the dynamical event. The most unambiguous set of states for expanding an electronic wave function is the set of *adiabatic* or *Born—Oppenheimer* electronic states that diagonalize the electronic Hamiltonian when the nuclear positions are fixed.[28-34] Finite nuclear velocities cause nonadiabatic transitions between these states.[7,8,32-35] Depending upon whether such a transition has or has not occurred, we classify processes (energy-transfer collisions and chemical reactions) as *electronically adiabatic* or *electronically nonadiabatic*. In semiclassical language, we envision the transition as corresponding to a *switch* from nuclear motion on one adiabatic potential energy surface to nuclear motion on another. In some semiclassical theories, such switches involve discontinuous changes in nuclear momenta, and they are also called *hops*. In general the potential *surfaces* are the sum of electronic energy and nuclear repulsion for a given electronic state and nuclear geometry. Technically these are energy hypersurfaces, but we usually just say "surfaces." The surfaces corresponding to the adiabatic electronic states are called adiabatic surfaces or *adiabats*.

The electronically adiabatic states are not the only possible basis for expanding the electronic wave function. In an accurate solution of the Schrödinger equation, the use of any basis leads to the same results for physical observables, but this is not true for approximate methods. Furthermore, some bases may be more efficient computationally or lead to more insight. For example, one is often intereseted in transitions between covalent (A:BC) and ionic (A⁺BC⁻) states, where we have used *valence bond* language to label the states. The ionic state may be the second adiabatic state for A far from BC, but it may be the first (lowest-energy) adiabatic state for tight geometries or for products A⁺B⁻ + C). Thus the valence bond labeling is not in one-to-one correspondence with the adiabatic labeling, and there must be *surface crossings* (places where two surfaces are equal) of the valence bond states along the reaction path. Near the surface crossings, if the adiabatic states are written as linear combina-

tions of the valence bond states, there will be appreciable weights for more than one of them. As the system passes the crossing, the weights shift relatively rapidly, for example, from (1, 0) toward (0, 1). The nuclear momentum operator (which is a derivative operator in nuclear coordinates) acting on these weights causes a large coupling, so the system may or may not stay in the same adiabatic electronic state. Under some conditions it may be most probable that the valence bond character does not change, corresponding to a nonadiabatic transition between adiabatic states. In such a case it may be more physical to use a valence-bond-like basis. A systematic way to do this is to use a *diabatic basis*. Whereas adiabatic states diagonalize the electronic Hamiltonian but are coupled by nuclear momentum, diabatic states have no nuclear momentum coupling but are coupled by off-diagonal elements (U_{12}) of the electronic Hamiltonian. Thus the coupling is a vector (called d_{12}) in an adiabatic representation but a scalar in a diabatic one. We hasten to point out that although exact adiabatic states exist in principle, exact diabatic states do not exist[36] (because in general one cannot make all components of d_{12} vanish simultaneously). In practice we per force use approximate adiabatic states (because of computational limitations), and we also use approximate diabatic states (because exact diabatic states do not exist). We note that the adiabatic potential surfaces are called V_1 and V_2, and they are the eigenvalues of the diabatic potential surface matrix

$$\begin{pmatrix} U_{11} & U_{12} \\ U_{12} & U_{22} \end{pmatrix}$$

The diagonals of this matrix are called diabatic surfaces or *diabats*. The precise methods that can be used to create an approximate diabatic basis are discussed elsewhere[28,33,36-48] and will not be reviewed here. Instead we are interested in how well the questions of whether more accurate results can be obtained by solving the semiclassical problem of coupled nuclear motion and electronic state evolution in a diabatic representation or an adiabatic representation and what is the best semiclassical method for calculating such results.

Crossings of the adiabatic states are less frequent than diabatic crossings. When U_{12} is zero by symmetry, the adiabats and diabats are the same (a case not considered further in this article), but when U_{12} can be nonzero, diabats can cross in a space of dimension $F - 1$ (where F is the number of internal degrees of freedom, equal to 3 for triatomics), whereas adiabats can cross in a space of dimension $F - 2$. Such adiabatic crossings are called *conical intersections*.[28-31,49,50]

II. Review of Methods

The semiclassical methods considered here are all trajectory-based methods including the full dimensionality of the system. We consider two different classes of methods: the trajectory surface-hopping (TSH) approach[8,35,51-54] and the self-consistent potential (SCP) approach.[19,55-61] Both of these approaches may be thought of as versions of the time-dependent-self-consistent field (TDSCF) method. For example, the TSH method may be derived by requiring that in the limit of degenerate potential surfaces the number of trajectories that are propagating on a given potential surface at any given time is proportional to the average of the diagonal electronic density matrix element corresponding to that surface. The self-consistency of the surface governing nuclear motion with the electronic density matrix is thus obtained for the entire ensemble, in that limit. The SCP method may also be employed with an average over an ensemble of trajectories,[59-61] but most work has involved more practical versions[19,55-58] in which the potential energy governing the

Feature Article

J. Phys. Chem. A, Vol. 104, No. 34, 2000 **7919**

motion of a single trajectory is consistent with the electronic density matrix elements calculated along that trajectory. That is, self-consistency is obtained for each trajectory individually and independent of the other trajectories. In this section we review one example of each type of method for the case of two electronic states. In particular, we review the Tully's fewest switches (TFS)[52] version of TSH, and we review the Ehrenfest version[19,55] of SCP. In other work we tested[19,21-23] another surface-hopping method, the Blais—Truhlar method,[51] and we tested[22,23] an alternate SCP method, the classical electron method[55] of Meyer and Miller. Both methods have serious shortcomings. Although the Blais—Truhlar method predicts reasonable probabilities of producing nonadiabatic products for systems with strong electronic coupling, it typically predicts zero chance of forming these products for systems with weak electronic coupling.[23] The classical electron method, because of a Langer-type[62] modification, often populates closed electronic states and tends to predict final rotational and vibrational moments that are too large.[22,27] Since Tully argued that surface hopping is not compatible with a diabatic representation,[8] and since the Ehrenfest method is independent of representation, and since the fewest switches and Ehrenfest algorithm perform better than the Blais—Truhlar and classical electron algorithms, we take the TFS surface-hopping method in the adiabatic representation and the Ehrenfest self-consistent potential method to be the standard representatives of their classes.

In this section we also review improvements in each of the two representative semiclassical methods. For the TFS method, the improvement is a criterion for selecting between adiabatic and diabatic representations to find the one that leads to the more accurate results. For the Ehrenfest method, the improvement is a method to include decoherence so that trajectories finish in a pure state when they leave the region where the states are coupled; the improved Ehrenfest method is called continuous surface switching.

In all of the semiclassical trajectory methods that we consider, a distinction is made between quantum variables, r, and classical variables, R. The classical variables are assumed to be described by classical trajectories $R(t)$, and the quantum variables are described by the time-dependent Schrödinger equation. For the case of two electronic states, the electronic wave function is given by

$$\Phi(R(t); r) = c_1(t) \phi_1(r; R(t)) + c_2(t) \phi_2(r; R(t)) \quad (1)$$

where ϕ_i is a basis function, the coefficients evolve according to[35]

$$\dot{c}_1(t) = -c_2(t)\left[\frac{i}{\hbar}H_{12}(R) + \dot{R}\cdot d_{12}(R)\right]\frac{\eta_1(t)}{\eta_2(t)} \quad (2)$$

$$\dot{c}_2(t) = -c_1(t)\left[\frac{i}{\hbar}H_{21}(R) + \dot{R}\cdot d_{21}(R)\right]\frac{\eta_2(t)}{\eta_1(t)} \quad (3)$$

where

$$\eta_i(t) = \exp\left(-\frac{i}{\hbar}\int^t H_{ii}(R)\,dt\right) \quad (4)$$

$$H_{kj}(R) = \langle\phi_k(r; R)|H_{el}(r; R)|\phi_j(r; R)\rangle \quad (5)$$

$$d_{kj}(R) = \langle\phi_k(r; R)|\nabla_R\phi_j(r; R)\rangle \quad (6)$$

and H_{el} is the electronic Hamiltonian. In a diabatic basis, $H_{ij} = U_{ij}$ and $d_{ij} = 0$. In an adiabatic basis $H_{ii} = V_i$ and $H_{ij} = 0$.

Instead of working with the coefficients c_1 and c_2, it is often convenient to use the electronic density matrix

$$\begin{pmatrix} \rho_{11} & \rho_{12} \\ \rho_{21} & \rho_{22} \end{pmatrix} = \begin{pmatrix} |c_1|^2 & c_1^*c_2 \\ c_2^*c_1 & |c_2|^2 \end{pmatrix} \quad (7)$$

where the diagonal elements are the populations of the states and the off-diagonal elements are the electronic coherences. It can be seen in eqs 2 and 3 that the choice of the classical trajectory determines the evolution of the quantum wave function. In both the trajectory surface-hopping methods and self-consistent potential methods the electronic density matrix elements are used to self-consistently determine the paths of the classical trajectories, although each method accomplishes this in a different fashion.

II.A. TFS Method. The TFS method is the surface-hopping method that has the fewest number of surface switches necessary to obtain ensemble-averaged consistency between the quantum and the classical degrees of freedom in the limit of $H_{11}(R) = H_{22}(R)$. (Of course, the surfaces are never degenerate for all R, but it is only in this limiting case that surface hopping can ever be self-consistent, so the limiting case is used to derive the method.) Self-consistency is accomplished by propagating an ensemble of trajectories on the diagonal potential matrix elements, with each trajectory being independent of the others. The probability that a trajectory that is propagating on potential surface $H_{ii}(R)$ at a time t_1 will hop to surface $H_{jj}(R)$ at time t_2 is given by

$$P_{i \rightarrow j} = \max\left[\frac{\rho_{ii}(t_1) - \rho_{ii}(t_2)}{\rho_{ii}(t_1)}, 0\right] \quad (8)$$

The results of TSH methods depend on the choice of the vector used to adjust the nuclear momentum during surface hops. We have tested two difference choices for the hopping vector: the gradient of the difference of the adiabatic potential energies and the nonadiabatic coupling vector. We have typically found that the results are not too sensitive to this choice[21] when hops occur in regions of strong nonadiabatic coupling, as both vectors point in nearly the same direction in these regions. In regions of weaker nonadiabatic coupling, when the two vectors do point in somewhat different directions, the nonadiabatic coupling vector was found to give better results.[24] Furthermore, the nonadiabatic coupling vector is the choice suggested by semiclassical analogies,[8,63] and therefore this is the choice we make for the present work.

In practice, the self-consistency of the TFS method may be violated. One reason for this is that hops from the lower surface to the upper surface may be energetically forbidden. More generally, there may be insufficient momentum along the vector that is used to adjust the momentum to allow a hop to occur. Either of these happenstances is called a frustrated hop. The procedures we have used in these cases are, in the first case, to continue propagating on the initial surface with no momentum discontinuity and, in the more general case, to reverse the component of the momentum that lies along the hopping vector. (This follows from a model[6,64] in which a single potential surface corresponds to one or the other of H_{11} and H_{22} on the two sides of a hopping seam). An alternate procedure advocated in the literature[65] is to treat both cases the first way. Although we have not tested this alternate procedure for strongly coupled systems, we have found that for very weakly coupled systems the errors are slightly smaller for this alternate procedure than for the first procedure discussed,[66] and this remains an area of investigation.

Another suggestion to remedy the problem of frustrated surface hops in the adiabatic representation is to replace the velocity in eqs 2 and 3 with an average velocity that points in the direction of the velocity on the surface the trajectory is currently being propagated on and has the magnitude of the geometric mean of the velocities the trajectory would have if propagated on either potential surface.[67] Energetically prohibited hops will not occur in this prescription, since when the kinetic energy on the upper surface becomes zero the coefficients $c_1(t)$ and $c_2(t)$ will be constant and no hops will occur. However, we have found that this procedure systematically increases the total nonadiabatic probability.[66] This is probably because such a treatment increases the rate at which $c_2(t)$ changes with time (by mixing in ground-state kinetic energy) and decreases the rate at which $c_1(t)$ changes with time (by mixing in excited-state kinetic energy character). Furthermore, such a treatment is not applicable to trajectory propagation in the diabatic representation because in that case the coupling is not an explicit function of velocity.

Alternate forms for the hopping vector were introduced in an earlier work[24] in an attempt to improve the poor self-consistency of the TFS method resulting from momentum-prohibited surface hops. These vectors were obtained by rotating the hopping vector toward the momentum vector by the smallest amount necessary to allow a hop to occur. However, these rotated vectors were found to give poorer internal energy distributions than the nonrotated hopping vectors and so will not be considered further here.

II.B. Choice of Representation for the TFS Method. The results of the TSH calculations depend on the representation (adiabatic or diabatic) of the electronic basis functions. This is a drawback of the method; the ideal semiclassical method should share with accurate quantum mechanics the invariance of the results to the choice of basis functions. However, since the results do depend on the choice of basis functions, we want to use the basis functions that yield the most accurate results. We have shown in earlier work[26] that there is a correlation between the representation in which the TSH calculations are most accurate and the number of times that trajectories switch surfaces. We anticipate, however, that although a small number of successful hops may occur in one representation, the self-consistency of the TFS method in that representation may be poor if a large number of frustrated hops occur. In this work therefore we modify our strategy; in particular we now select the representation in which the fewest number of surface-hop attempts occur. Note that for the two cases we studied previously[26] both the minimum surface-hop criterion and the minimum surface-hop-attempt criterion yield the same choice of representation, although in general this will not be the case. We label the representation that our new criterion selects the Calaveras County representation after the location where strategies were devised to keep a well-known frog from attempting a hop,[68] and we present TFS results for this representation in addition to the adiabatic and diabatic representations. For the sake of brevity this representation may also be referred to as the least hopping attempts (LHA) representation. Note that for an ensemble of trajectories beginning in a single initial state the Calaveras County representation will give the same results as either the adiabatic or the diabatic representation. However, for results that are averages over several initial states, the results of using the Calaveras County representation will not be equivalent to either the adiabatic or diabatic representations as the Calaveras County representation may change for different initial states.

Other criteria for selecting the proper representation to perform TFS calculations in have been reviewed elsewhere[26] and will not be mentioned here. We have found that the hop-attempt minimizing criterion that defines the Calaveras County representation is better than the others we have examined.

It is also possible that there is some representation that is neither adiabatic nor diabatic in which TFS calculations agree even better with quantum results than either the adiabatic or the diabatic representation. This has been examined in more detail elsewhere[69] and is a worthwhile subject for further study.

II.C. Ehrenfest Method. In the Ehrenfest method the potential energy is given by the expectation value of the electronic Hamiltonian

$$H_E(R) = \langle \Phi(r; R)|H_{el}(r; R(t))|\Phi(r; R) \rangle \qquad (9)$$

where Φ is the electronic wave function of eq 1. The Ehrenfest method is independent of the choice of representation of the electronic basis functions,[55] and it avoids several other undesirable feature of the TSH methods as well. Since surface hops do not occur, use of the Ehrenfest method avoids having to determine along which direction the momentum should be adjusted during a surface hop. The Ehrenfest method also always maintains its self-consistency since there are no frustrated hops. The biggest drawback of this method is that trajectories propagating according to eq 9 may finish on a mixed state that is not an eigenvalue of the asymptotic electronic Hamiltonian. This is as much a practical difficulty as it is a formal one; trajectories that leave the interaction region on a mixed potential surface will not have the correct internal energy distributions. Furthermore, if for a particular asymptotic arrangement one of the diagonal potential matrix elements of eq 5 is very energetically inaccessible, then the potential energy defined by eq 9 will almost always be energetically inaccessible, and the Ehrenfest method may predict zero probability of ending in that arrangement even though there is a dynamically accessible surface.

II.D. An Improved Self-Consistent Potential Method: The CSS Method. Recently, we presented a new self-consistent potential method called the continuous surface-switching (CSS) method in which the mixed state is resolved into one or the other pure electronic state as the trajectory leaves the region of interstate coupling.[27] This resolution is accomplished in such a way that the probability of finishing on a given surface, when averaged over an ensemble of trajectories, is consistent with the average electronic density matrix elements. Thus the method is still self-consistent, but in an ensemble-average sense rather than trajectory by trajectory. We may also think of CSS as a type of surface-hopping method in which the surface hops are replaced by switches that occur continuously in time.

Substituting eq 1 into eq 9 gives

$$H_E(R) = \sum_i \sum_j w_{ij}(\rho_{ij}) H_{ij}(R) \qquad (10)$$

where $w_{ij}(\rho_{ij}) = \rho_{ij}$. The essence of the CSS methods is to allow the weights w_{ij} to be more general functions of ρ_{ij}. In particular, we leave the off-diagonal weights w_{ij} unchanged, but we define the diagonal weights w_{ii} so that they approach the density elements ρ_{ii} in regions of strong coupling but go to either 0 or 1 in asymptotic regions. The precise form of the function used to determine the weights is somewhat arbitrary and remains a topic of research. We note, however, that the TFS method, while quite successful, also involves a degree of arbitrariness in the selection of the fewest switches criterion. One reason to prefer this criterion is simplicity,[52] and we used a similar guide in the

Feature Article

J. Phys. Chem. A, Vol. 104, No. 34, 2000 **7921**

selection of our functions for w_{11} and w_{22} in our initial tests of the CSS method.[27]

In general, CSS calculations could be carried out in either an adiabatic or a diabatic representation, although so far we have only tested the latter. However, in regions of strong interstate coupling the method becomes equivalent to the Ehrenfest method, which is independent of representation, and in regions of weak interstate coupling the diabatic and adiabatic representations are very similar. Therefore the CSS method has been designed in such a way that it will be less sensitive to the choice of electronic representation than the TSH method.

II.E. Final-State Assignment. A general problem in all trajectory calculations is that the classical values of the vibrational and rotational quantum numbers are not automatically integers. As discussed above, a similar problem occurs in the Ehrenfest method for the electronic quantum number, but for the TSH and CSS methods, the final electronic quantum number is assigned on the basis of the surface in which the trajectory finishes.

For all calculations used to compute mean unsigned errors in this paper, the final vibrational and rotational quantum numbers v and j were assigned by the linear smooth sampling (LSS)[6,22,70–72] algorithm. In this algorithm, each trajectory contributes to the four discrete v, j states that bracket the final continuous numbers resulting from the trajectory calculation. The weight of each of these discrete v or j values is a linear function of the closeness of the continuous variable to the discrete values. For TSH and CSS trajectories, each trajectory contributes to four final states (two vibrational quantum numbers × two rotational quantum numbers), while for the Ehrenfest method each trajectory contributes to eight final states (two vibrational × two rotational × two electronic). Two other methods for assigning the final-state variables that we have previously tested are the histogramming[6,22] algorithm and the quadratic smooth sampling (QSS) algorithm.[16,73] In the histogramming method each of a trajectory's final continuous quantum numbers is simply rounded to the nearest discrete quantum number. The QSS method is similar to the LSS method except that the weight is a quadratic function of the closeness of the continuous variable to the nearest discrete quantum state.

Since every Ehrenfest trajectory finishes in an electronic state that is a mixture of the two pure states, it seems natural that in the assignment of the electronic variable every trajectory should contribute to final dynamical quantities associated with both electronic states. The LSS and QSS algorithms accomplish this; the histogramming algorithm does not. With no particular reason to prefer one of the smooth sampling methods to the other, we select LSS for its simplicity. We have typically found, however, that all three of these procedures result in similar predictions for the final dynamical quantities (although one exception to this is described in a later section). For consistency, we chose to use LSS for all of our trajectory methods and all three (vibrational, rotational, and electronic) sets of quantum numbers.

In some cases, especially for the Ehrenfest method, this procedure results in trajectories being assigned to states whose energies exceed the total energy of calculation. We have explored the possibility of reassigning these trajectories to lower-energy states but have found that this generally decreases the overall accuracy of the calculation,[22] and so we do not use this reassignment procedure in the present review.

III. Examples

In this section we review the systems for which we have performed both quantum mechanical dynamics calculations and

semiclassical calculations. All of the systems we discuss are three-body systems performed without any dimensionality-reducing assumptions (such as collinear collisions or spherical interaction potentials); however, we consistently omit electronic angular momentum and electronic Coriolis coupling, and we consider only zero total angular momentum. All of the systems have realistic two-state potential energy matrices defined in the diabatic representation (the adiabatic potential surfaces are obtained when necessary by diagonalization). The symbols used in our tables and in our discussion are defined by the following equations

$$A^* + BC(v,j) \rightarrow A + BC(v'',j'') \qquad (Q)$$

$$\rightarrow AB(v',j') + C \qquad (R)$$

or

$$ABC^* \rightarrow A + BC(v'',j'') \qquad (D)$$
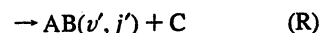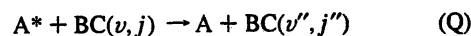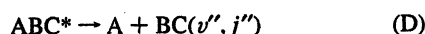
where an asterisk denotes electronic excitation. The quantities v and j are the final rotational and vibrational quantum numbers, with primes distinguishing nuclear arrangements. The probability of process Q is called the quenching probability, P_Q, and the probability of process R is called the reaction probability, P_R. Although the unimolecular decomposition process labeled by D may be thought of as a photodissociation reaction, we have in other work[24,26] referred to this as a quenching process since the species ABC* is excited and the products are not, and we continue to use this description in the present review.

The NaH$_2$ system was studied at energies where the NaH + H arrangement was inaccessible. This is a large gap system; the Na excitation energy is 2.1 eV. We studied two parametrizations of this system (5F[9,42] and 6[47]); differences have been discussed elsewhere.[47] NaH$_2$ has a line of conical intersections at C_{2v} geometries, and it is accessible in both parametrizations; however, it is more readily accessible for the 5F case than in case 6.

We studied two different parametrizations of the MHH system, where M is a model metal with an excitation energy of 0.76 eV. In this system the product MH + H arrangement is energetically accessible. The two different parametrizations are otherwise similar to the NaH$_2$ system; they differ from each other in that one of them (parametrization 1)[21] the M* + H$_2$ → MH + H reaction is exothermic, while in the other (parametrization 2)[22] it is endothermic.

We also studied reactions in the MXH system, where M is a model metal and X is a model halogen atom. These systems do not have conical intersections, but they do have avoided crossings (i.e., the diabats do cross, but the diabatic crossing seam does not intersect a region where $U_{12} = 0$). We studied three parametrizations of this system;[47] they differ in the strength and broadness of the U_{12} coupling surface and are labeled WL, SL, and SB. The first letter represents the strength of the diabatic coupling element U_{12} (strong or weak) and the second letter represents the spatial extent of the diabatic coupling (localized or broad).

The last system we examined is the BrH$_2$ system.[16,74] This system has a small excitation energy (0.5 eV), and in this system neither the adiabats nor the diabats cross.

The differences in the systems that we studied are pictured in Figure 1. Panels a, c, and e illustrate the diabatic matrix elements, while panels b, d, and f illustrate the adiabatic curves. Panels a and b show MHH parametrization 1, in which both diabats and adiabats cross. Panels c and d show MXH parametrization SL, in which diabats cross but adiabats avoid
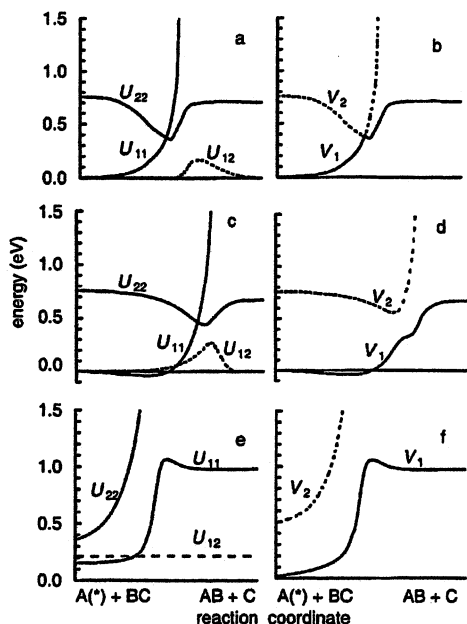
7922 *J. Phys. Chem. A, Vol. 104, No. 34, 2000*

Hack and Truhlar

Figure 1. Schematics of several potential energy surfaces for A or A* + BC → AB + C. (a) Diabatic matrix elements for MHH parametrization 1. (b) Adiabatic matrix elements for MHH parametrization 1. (c) Diabatic matrix elements for MXH parametrization SL. (d) Adiabatic matrix elements for MXH parametrization SL. (e) Diabatic matrix elements for the BrH_2 system. (f) Adiabatic matrix elements for the BrH_2 system.

crossing, i.e., there is no conical intersection. Panel d shows how the adiabatic curves are not as smooth as the diabatic ones. This, plus the economy of the coupling being a scalar rather than a vector, is one of the motivations for modeling systems diabatically. Panels e and f illustrate the BrH_2 system, in which neither the adiabats nor the diabats cross. The NaH_2 parametrizations are similar to panels a and b except that the product arrangement opens at 2.8 eV while the excitation energy of Na is 2.1 eV.

For all of the systems described above except for parametrization 6 of the NaH_2 system we performed bimolecular collision calculations, and for the two parametrizations of the NaH_2 system we also performed unimolecular decay calculations.

This collection of eight systems and reactions, while not exhaustive in the number of different possible types of nonadiabatic processes, does constitute a test set with a variety of different surface types for comparing approximate semiclassical methods to accurate quantum mechanical calculations.

IV. Discussion of Results

For all eight cases, we calculated errors in the quenching probability, the reaction probability (where applicable), and the final vibrational and rotational quantum numbers of the final diatomic fragments. The errors in the probabilities and final vibrational and rotational quantum numbers were calculated by comparing to the results of converged quantum dynamics calculations. For some of the systems (see original papers[19,21-24,26,27]) we considered several system energies and/or initial states, and in such cases the mean absolute errors are averaged over all energies and initial states. For NaH_2, MHH, and MXH, the results are further averaged over the two or three parametrizations of that type. The mean unsigned errors (i.e., mean absolute deviations from accurate quantal results) are summarized in Table 1.

TABLE 1: Mean Unsigned Errors[e]

	P_R	P_Q	$\langle v' \rangle$	$\langle j' \rangle$	$\langle v'' \rangle$	$\langle j'' \rangle$
NaH_2[a] (Two Parametrizations)						
TFS—adiabatic	—	0.23	—	—	0.27	**1.0**
TFS—diabatic	—	**0.12**	—	—	0.27	1.2
TFS—Calaveras Co.	—	0.23	—	—	**0.18**	1.0
Ehrenfest	—	0.48	—	—	0.52	2.1
MHH[b] (Two Parametrizations)						
TFS—adiabatic	0.12	0.10	0.05	1.2	0.14	1.0
TFS—diabatic	0.13	**0.07**	0.04	**1.1**	0.11	0.9
TFS—Calaveras Co.	**0.10**	0.08	0.04	1.2	**0.09**	**0.8**
Ehrenfest	0.24	0.20	0.08	1.3	0.16	1.8
BrH_2[c] (One Parametrization)						
TFS—adiabatic	6.9×10^{-4}	3.5×10^{-3}	0.14	2.4	**0.38**	**0.8**
Ehrenfest	6.1×10^{-4}	3.7×10^{-3}	**0.00**	6.7	0.85	1.0
MXH[d] (Three Parametrizations)						
TFS—adiabatic	0.25	0.08	**0.07**	1.0	**0.08**	**0.6**
TFS—diabatic	0.21	0.11	**0.07**	0.8	0.14	0.7
TFS—Calaveras Co.	0.26	**0.07**	0.08	0.9	**0.08**	**0.6**
Ehrenfest	0.20	0.12	0.16	1.6	0.21	1.0
CSS	**0.09**	0.11	0.10	0.9	0.22	**0.6**

[a] From refs 9, 42, 47. [b] From refs 21, 22. [c] From refs 16, 74. [d] From ref 27. [e] Bold numbers indicate the best method for the dynamical quantity. Column headers are defined in section III.
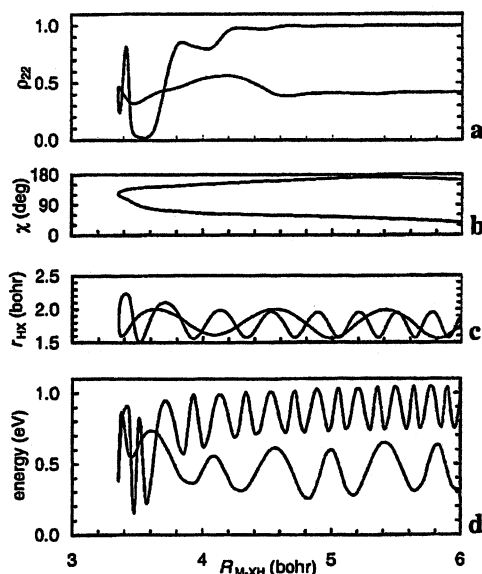

Figure 2. Ehrenfest trajectory undergoing a quenching process as a function of the distance R_{M-HX} between M and the center of mass of HX. This trajectory was calculated at 1.1 eV from the $v = 0, j = 0$ initial state on parametrization SL of the MXH system. (a) ρ_{22}. (b) The Jacobi angle χ, which is the angle between the M−HX vector and the HX vector. (c) The HX bond length r_{HX}. (d) The potential energy.

IV.A. What Goes Wrong? The most serious drawback of the Ehrenfest is that the potential energy defined by eq 9 does not become equal to one of the pure potential energy surfaces when the trajectory leaves the region of interaction. This is illustrated more clearly in Figure 2, which describes an Ehrenfest trajectory undergoing a quenching process. Note that all of the plotted quantities are smooth functions of R_{M-HX}. However, the trajectory ends in a mixed state with $\rho_{22} = 0.42$; in panel d it can be seen that the minimum potential energy along the exit path is 0.32 eV, instead of 0 or 0.76 eV as it would be if the trajectory finished in a pure ground or excited state, respectively. A consequence of the unquantized electronic energy is that the final vibrational−rotational energy distribution does not re-
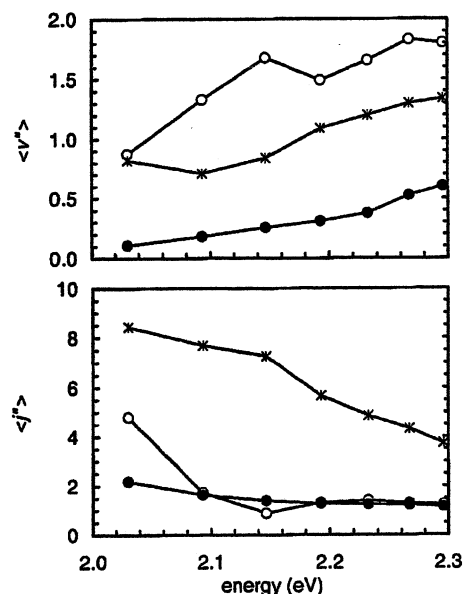
Feature Article

J. Phys. Chem. A, Vol. 104, No. 34, 2000 **7923**

Figure 3. Final average final quantum numbers of H_2 for the unimolecular decay of NaH_2 in parametrization 6 as functions of total energy of the system. The asterisks represent the accurate quantum mechanical results, the filled circles represent the Ehrenfest results with final states assigned using the LSS method, and the open circles represent the Ehrenfest results with final states assigned by histogramming. (a) Final vibrational quantum number. (b) Final rotational quantum number.

semble that for either possible electronic state of M + HX. As a corollary, the Ehrenfest method is more sensitive than other methods to the scheme used to assign final quantum states. For example, for NaH_2 with the LSS algorithm, the results could have contributions from trajectories whose energies are adjusted by over 2 eV.

An illustration of the final-state assignment problem for the Ehrenfest method is shown in Figure 3a, where we have plotted the final average vibrational quantum number for the diatomic fragments resulting from the unimolecular decay of an initially excited NaH_2 exciplex in parametrization 6. Notice that the results of using histogramming to assign the product vibrational quantum numbers and using LSS to do the assigning are very different.

Figure 3b illustrates another problem with the Ehrenfest method, which is that the final internal energies associated with small-probability pathways will have large errors. This is because the Ehrenfest potential energy surface will mainly resemble the pure-state surface of the large-probability pathway. In parametrization 6 of the NaH_2 system the large-probability pathway is the excited-state surface, which is characterized by an attractive exciplex, and the small-probability pathway is the ground-state surface, which is repulsive. Predictions of the Ehrenfest method for the internal energy distribution for the ground-state products in this system have a large error because trajectories leave the interaction region under the influence of the wrong physical forces. Table 1 illustrates this point further; the Ehrenfest method typically has an error in the final vibrational and rotational quantum numbers that is twice that of the TFS methods.

Another related error is that the mixed character of the potential energy often results in systematically low estimations of the reaction probability for arrangements in which the excited-state potential surface is energetically inaccessible. This occurs

TABLE 2: Average Mean Signed Errors in the Reaction Probabilities for the Ehrenfest, CSS, and TFS Calculations in All Three Representations

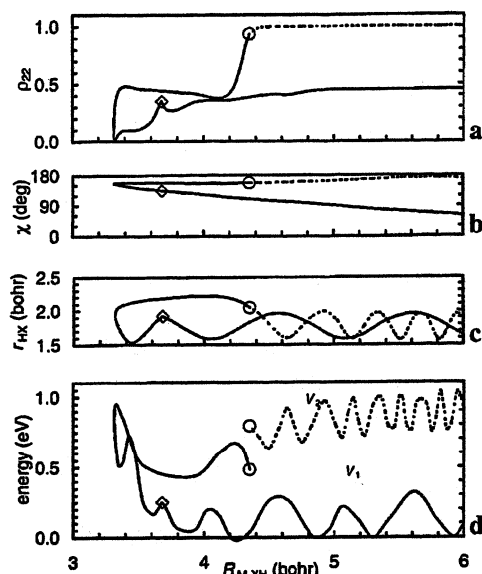| system	Ehrenfest	CSS	TFS diabatic	TFS adiabatic	TFS Calaveras Co.
MHH 1	−0.20	−	0.08	−0.10	0.02
MHH 2	−0.28	−	−0.06	−0.08	−0.08
MXH WL	−0.20	−0.09	0.21	0.23	0.21
MXH SL	−0.17	0.03	0.26	0.32	0.32
MXH SB	−0.22	−0.02	0.13	0.20	0.20
BrH_2	-6.2×10^{-4}	−	−	5.6×10^{-4}	
Average Over:					
MXH systems	−0.20	−0.03	0.20	0.25	0.24
all systems	−0.15	−0.03	0.12	0.11	0.13

Figure 4. TFS trajectory in the Calaveras Co. representation (which, in this case, is the adiabatic one) undergoing a quenching process. The initial conditions of the trajectory are the same as for Figure 2. In these panels, an open circle indicates the location of a surface hop, and an open diamond indicates the location of a hop attempt that was frustrated owing to insufficient momentum along the **d** vector. In each panel the dashed line represents propagation in the excited state and the solid line represents propagation on the ground state. (a) ρ_{22}. (b) The Jacobi angle χ. (c) The HX bond length (r_{HX}). (d) The potential energy.

when reaction is a small-probability event and the Ehrenfest potential has a large contribution from an energetically closed excited surface. This is illustrated in Table 2 for the cases involving a chemical reaction. Notice that in every case the reaction probability is below the accurate quantum estimation. The TFS methods by contrast predict a reaction probability that is too high on average, although there is not as systematic a trend for the TFS methods as there is for the Ehrenfest method.

The TFS method also has undesirable characteristics. Figure 4 illustrates a trajectory calculated with the TFS method in the Calaveras Co. representation for parametrization SL of the MXH system. Note the location of the surface hop and the subsequent change in the motion of the trajectory, illustrated in panels c and d. One of the assumptions in the derivation of the fewest switches trajectory surface-hopping algorithm is that trajectories should follow paths that are independent of the surface being used to propagate them; the change in character at the location of the open circle clearly illustrates that this requirement is not being satisfied in this case. The diamond illustrates a hop attempt
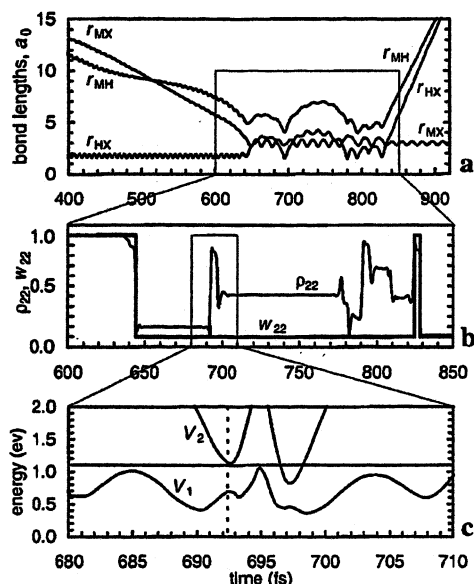
Figure 5. Reactive TFS trajectory in the Calaveras Co. representation (which, in this case, is the adiabatic one) for the initial conditions described in Figure 2. (a) The three bond lengths as a function of time. (b) The thin line represents ρ_{22}, and the thick line represents the weight w_{22} of the excited-state surface. The thick vertical lines represent surface hops. (c) The potential energy of the ground- and excited-state adiabatic potential energy surfaces. The vertical dashed line represents the location of an energetically frustrated surface-hop attempt.

that was frustrated owing to insufficient momentum along the **d** vector. Panel a illustrates the sharp change in the evolution of ρ_{22} resulting from reversing the momentum component that lies along **d**. The effect of this momentum reversal can also be seen by the sharp change in the HX vibrational motion in panel c and in the potential energy in panel d. Although we have never seen evidence of a systematic difference in final average dynamical quantities between reversing the momentum component along **d** in the case of a momentum-prohibited hop or not carrying out such a reversal, the sharp change in the evolution of ρ_{22} resulting from this procedure suggests that allowing the momentum to remain unchanged may be a more physical alternative, although it does not follow from the model mentioned in section II.A.

Figure 5 illustrates a reactive TFS trajectory in the Calaveras Co. representation as a function of time. Panel a illustrates the evolution of the bond lengths with time. The interaction period occurs between about 600 and 850 fs and is shown in more detail in panel b. It can be seen in panel b that three successful surface hops occur. In each case there is a corresponding change in ρ_{22}. Figure 5 also illustrates the stochastic nature of surface-hopping, namely, that not every large change in ρ_{22} causes a hop to occur. Panel b illustrates an energetically frustrated hop at 692 fs. At this time there is a rapid increase in ρ_{22}, but there is insufficient energy for a hop to occur as shown in panel c.

The most serious difficulty with the TFS method is the issue of representation. The adiabatic and the diabatic representations will have different forms of interstate coupling, and thus hopping between surfaces is likely to occur at different places and at different times. This is illustrated in Figure 6, where the lifetime of the NaH₂ excited-state complex with parametrization 6 is plotted versus total energy. In the diabatic representation surface hops occur more frequently,[26] and once trajectories hop to the lower repulsive surface, they rapidly dissociate before they can
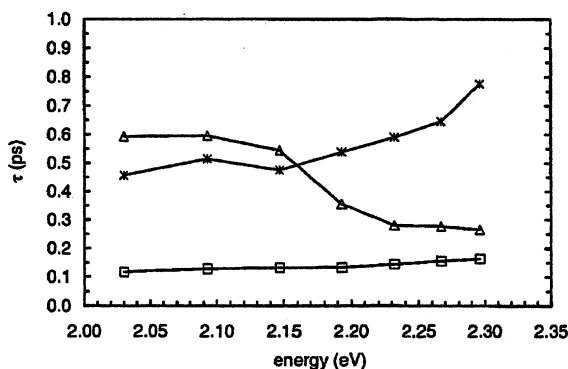

Figure 6. Lifetime of the NaH₂ exciplex calculated on NaH₂ parametrization 6. The open triangles represent the TFS results in the adiabatic representation, the open squares represent the TFS results in the diabatic representation, and the stars represent the quantum mechanical results.

hop back to the upper surface. This results in a prediction of shorter lifetimes than calculations in the adiabatic representation predict.

The worst-case examples for both TFS and the Ehrenfest method come from our calculations on the NaH₂ system. In the trivial case of degenerate states, both the Ehrenfest method and the TFS methods give identical vibrational—rotational distributions and reaction probabilities and all of the error in the calculation results from the classical treatment of the particles. It is thus large-gap systems in which the treatment of nonadiabatic effects becomes most important. NaH₂ is the largest gap system we have examined; for example, the potential energy gap for surface-hopping trajectories for parametrization 6 is often larger than 1 eV.[26] Thus the failures of each method are clearly illustrated by this system. Organic photochemistry often involves even larger gaps, e.g., the $n \rightarrow \pi^*$ excitation energy of acetone is 4.5 eV, and it is important to have accurate methods for the large-gap regime.

IV.B. What Goes Right? Figure 7 illustrates a CSS trajectory undergoing a quenching process. Panel a illustrates the values of ρ_{22} and w_{22} as functions of the M−HX center-of-mass distance. Note that w_{22} closely tracks ρ_{22} until the R_{M-HX} distance reaches 4.0 bohr, at which point w_{22} gradually goes to zero. This is further illustrated in panel d, where now the discretization of w_{22} allows the minimum energy in the vibration of HX to go to zero.

Table 1 shows that the CSS method has average errors in the six dynamical quantities that are smaller than the Ehrenfest method for the MXH systems. Table 2 shows that the CSS method corrects the tendency of the Ehrenfest method to give reaction probabilities that are too low. Thus it appears that forcing SCP trajectories to end in a quantized electronic state improves the observed dynamics.

It may appear from Table 1 as though the TFS results in the Calaveras County representation are not systematically better than the TFS results in either the adiabatic or the diabatic representation. However, for certain cases that we have examined the Calaveras County representation correctly describes the trends of dynamical quantities as a function of total energy whereas other representations do not (see, for example, ref 26 where the Calaveras County representation is equal to the adiabatic representation for NaH₂ parametrization 6, and it is equal to the diabatic representation for NaH₂ parametrization 5F). Figure 8 illustrates the reaction and quenching probability for two different initial states for parametrization 1 of the MHH
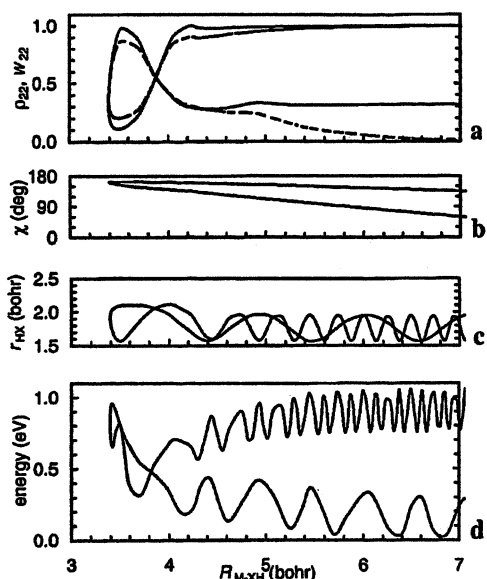
Feature Article

J. Phys. Chem. A, Vol. 104, No. 34, 2000 **7925**

Figure 7. CSS trajectory undergoing a quenching process for the initial conditions described in Figure 2. (a) The solid line represents ρ_{22}, and the dashed line represents w_{22}. (b) The Jacobi angle χ. (c) The HX bond length (r_{HX}). (d) The potential energy.
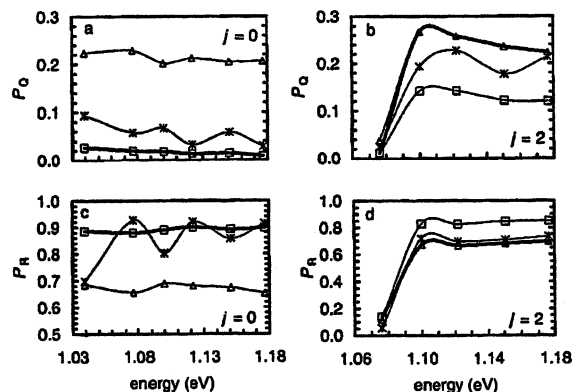

Figure 8. Reaction and quenching probability for parametrization 1 of the MH$_2$ system with H$_2$ initially in the $v = 0$ vibrational state. The open triangles represent the TFS results in the adiabatic representation, the open squares represent the TFS results in the diabatic representation, the stars represent the quantum mechanical results, and the solid line represents the TFS results in the Calaveras County representation. (a) The quenching probability for H$_2$ initially in the $j = 0$ rotational state. (b) The quenching probability for H$_2$ initially in the $j = 2$ rotational state. (c) The reaction probability for H$_2$ initially in the $j = 0$ rotational state. (d) The reaction probability for H$_2$ initially in the $j = 2$ rotational state.

TABLE 3: (Column I) Number of Cases (Defined in Section III) for Which Each Method Was within 20% of the Best Method for Each System and (Column II) Number of Cases for Which Each Method Had an Error Twice as Large as the Best Method for Each System

	I	II
NaH$_2$[a] (2 Parametrizations, 6 Cases)		
TFS—adiabatic	5	2
TFS—diabatic	5	2
TFS—Calaveras County	6	3
Ehrenfest	2	6
MHH[b] (2 Parametrizations, 12 Cases)		
TFS—adiabatic	6	2
TFS—diabatic	8	0
TFS—Calaveras County	9	0
Ehrenfest	4	7
BrH$_2$[c] (1 Parametrization, 6 Cases)		
TFS—adiabatic	5	1
Ehrenfest	4	2
MXH[d] (3 Parametrizations, 18 Cases)		
TFS—adiabatic	12	2
TFS—diabatic	11	4
TFS—Calaveras County	11	2
Ehrenfest	5	9
CSS	6	2

[a] From refs 9, 42, 47. [b] From refs 21, 22. [c] From refs 16, 74. [d] From ref 27.

system as a function of total energy. Clearly, the Calaveras County representation selects the best of either the adiabatic or diabatic representation. Note also that in this case the most accurate representation depends on the initial state. When the initial rotational quantum number is zero, the diabatic representation is most accurate, and when the initial rotational quantum number is two, the adiabatic representation is most accurate. The Calaveras County representation successfully predicts this trend.

The quenching probability for the NaH$_2$ systems is the one quantity for which the Calaveras County representation does not appear to be as good as the diabatic representation as seen in Table 1. The largest contribution to this error is from the

quenching probability for the unimolecular decay of NaH$_2$ in parametrization 6. In this case, the Calaveras County representation is the adiabatic representation, and 7 of the 10 energies that we studied were threshold energies that occurred above the classical asymptotic energy but below the asymptotic zero-point energy.[26] If we neglect these threshold energies in the calculation of the error, the error is reduced to 0.08 for all three TFS methods, and it is increased to 0.99 for the Ehrenfest method (the Ehrenfest method predicts less quenching because unlike the TFS methods, which must quench at energies below the classical asymptotic energy, Ehrenfest trajectories can always end up on a mixed surface and at low energies this surface closely resembles the excited-state surface). When one considers that in general semiclassical methods will have difficulty in threshold regions and in regions where zero-point energy conservation is important, the inaccuracy of the Calaveras County representation in this single case does not seem too severe.

In some cases, for instance, the MXH system and parametrization 2 of the MHH system, the TFS results do not depend significantly on representation, and of course the Calaveras County representation is as good as either of the other two representations.

We may gain insight into the robustness of a method by considering how many times it has the smallest error or an error that is very close to the smallest error (say within 20%) for all of the methods we consider, and how many times it has an error that is at least twice as large as the best method. Two of the systems that we have studied are characterized by three final dynamical quantities, and the remaining six systems are characterized by six dynamical quantities. This gives 42 cases for which we can compare methods. The number of cases for which each method is within 20% of the best and the number of times for which it has an error at least twice as large as the best are illustrated in Table 3. Table 3 shows that the TFS methods are very robust; that is, when they are not the best they still do not often have relatively large errors. This is in contrast to the Ehrenfest method, which although sometimes being the best, in many cases has an error relatively larger than

7926 *J. Phys. Chem. A, Vol. 104, No. 34, 2000*

Hack and Truhlar

the best method. Table 3 also shows that the CSS method is more robust than the Ehrenfest method. As mentioned in the original CSS paper[27] and above, large-gap systems will provide the most difficult tests for the CSS method, but also the best opportunity to demonstrate superiority. In these cases, the mixed-final-state problem of the Ehrenfest method will be more even more severe than for the examples given in section IV.A, and the CSS method should be even better by comparison.

V. Concluding Remarks

When only the overall, average errors are considered, there does not appear to be a method that systematically outperforms the others. However, when one examines dynamical quantities in greater detail the situation changes. The CSS method, for example, by removing the mixed-final-state aspect of the Ehrenfest method results in significantly reduced errors in the final internal energy (as characterized by the vibrational and rotational quantum numbers) and removes the systematically low probability of reaction of the Ehrenfest method. We expect these effects to be more significant for systems with larger energy gaps.

We also note that the TFS methods are very robust; for example, even when they are not the best method they still have relatively low errors. Furthermore, one of the largest drawbacks of the TFS methods, that of basis set dependence, may be somewhat alleviated by choosing the Calaveras County representation for surface hopping. When the results of calculations in the adiabatic and diabatic representations do not differ significantly, the Calaveras County representation is of course as good as either of the other systematic choices of representation. However, when the results do depend on representation, the Calaveras County representation tends to choose the most accurate representation, even when this optimum representation is a function of the initial state.

References and Notes

(1) Miller, W. H. *Adv. Chem. Phys.* **1974**, *25*, 69; **1975**, *30*, 77.

(2) Gentry, W. R. In *Atom-Molecule Collision Theory*; Bernstein, R. B., Ed.; Plenum: New York, 1979; p 391.

(3) Karplus, M.; Raff, L. M. *J. Chem. Phys.* **1964**, *41*, 1267.

(4) Bunker, D. L.; Blais, N. C. *J. Chem. Phys.* **1964**, *41*, 2377.

(5) Karplus, M.; Porter, R. N.; Sharma, R. D. *J. Chem. Phys.* **1965**, *43*, 3259.

(6) Truhlar, D. G.; Muckerman, J. T. In *Atom-Molecule Collision Theory*; Bernstein, R. B., Ed.; Plenum: New York, 1979; p 505.

(7) Child, M. S. In *Atom-Molecule Collision Theory*; Bernstein, R. B., Ed.; Plenum: New York, 1979; p 427.

(8) Tully, J. C. In *Modern Methods for Multidimensional Dynamics Computations in Chemistry*; Thompson, D. C., Ed.; World Scientific: Singapore, 1998; p 34.

(9) Schwenke, D. W.; Mielke, S. L.; Tawa, G. J.; Friedman, R. S.; Halvick, P.; Truhlar, D. G. *Chem. Phys. Lett.* **1993**, *203*, 565.

(10) Mielke, S. L.; Tawa, G. J.; Truhlar, D. G.; Schwenke, D. W. *J. Am. Chem. Soc.* **1993**, *115*, 6436.

(11) Mielke, S. L.; Tawa, G. J.; Truhlar, D. G.; Schwenke, D. W. *Int. J. Quantum Chem. Symp.* **1993**, *27*, 621.

(12) Tawa, G. J.; Mielke, S. L.; Schwenke, D. W.; Truhlar, D. G. *J. Chem. Phys.* **1994**, *100*, 5751.

(13) Gilibert, M.; Baer, M. *J. Phys. Chem.* **1994**, *98*, 12822.

(14) Gilibert, M.; Baer, M. *J. Phys. Chem.* **1995**, *99*, 5748.

(15) Schatz, G. C. *J. Chem. Phys.* **1995**, *99*, 7522.

(16) Mielke, S. L.; Tawa, G. J.; Truhlar, D. G.; Schwenke, D. W. *Chem. Phys. Lett.* **1995**, *234*, 57. Mielke, S. L.; Tawa, G. J.; Truhlar, D. G.; Schwenke, D. W. *J. Phys. Chem.* **1995**, *99*, 16210.

(17) Mielke, S. L.; Schwenke, D. W.; Truhlar, D. G. *J. Phys. Chem.* **1995**, *99*, 16210.

(18) Allison, T. C.; Mielke, S. L.; Schwenke, D. W.; Truhlar, D. G. *J. Chem. Soc., Faraday Trans.* **1997**, *93*, 825.

(19) Topaler, M. S.; Hack, M. D.; Allison, T. C.; Liu, Y.-P.; Mielke, S. L.; Schwenke, D. W.; Truhlar, D. G. *J. Chem. Phys.* **1997**, *106*, 8699.

(20) Last, I.; Giliber, M.; Baer, M. *J. Chem. Phys.* **1997**, *107*, 1451.

(21) Topaler, M. S.; Allison, T. C.; Schwenke, D. W.; Truhlar, D. G. *J. Phys. Chem. A* **1998**, *102*, 1666.

(22) Topaler, M. S.; Allison, T. C.; Schwenke, D. W.; Truhlar, D. G. *J. Chem. Phys.* **1998**, *109*, 3321; **1999**, *110*, 687 (E).

(23) Volobuev, Y. L.; Hack, M. D.; Truhlar, D. G.; Truhlar, J. *Phys. Chem. A* **1999**, *103*, 6225.

(24) Hack, M. D.; Jasper, A. W.; Volobuev, Y. L.; Schwenke, D. W.; Truhlar, D. G. *J. Phys. Chem. A* **1999**, *103*, 6309.

(25) Gray, S. K.; Petrongolo, C.; Drukker, K.; Schatz, G. C. *J. Phys. Chem. A* **1999**, *103*, 9448.

(26) Hack, M. D.; Jasper, A. W.; Volobuev, Y. L.; Schwenke, D. W.; Truhlar, D. G. *J. Phys. Chem. A* **2000**, *104*, 217.

(27) Volobuev, Y. L.; Hack, M. D.; Topaler, M. S.; Truhlar, D. G. *J. Chem. Phys.* **2000**, *112*, 9716.

(28) Salem, L. *Electrons in Chemical Reactions*; Wiley: New York, 1982.

(29) Simons, J. *Energetic Principles of Chemical Reactions*; Jones and Bartlett: Boston, MA, 1983.

(30) Michl, J.; Bonacic-Koutecky, V. *Electronic Aspects of Organic Photochemistry*; Wiley: New York, 1990.

(31) Michl, J. In *Theoretical and Computational Models for Organic Chemistry*; Formosinho, S. J., Csizmadia, I. G., Arnaut, L. G., Eds.; Kluwer: Dordrecht, 1991; p 207.

(32) Hirschfelder, J. O.; Meath, W. J. *Adv. Chem. Phys.* **1967**, *12*, 3.

(33) Garrett, B. C.; Truhlar, D. G. *Theor. Chem. Adv. Persp.* **1981**, *6A*, 216.

(34) Rebentrost, F. *Theor. Chem. Adv. Persp.* **1981**, *6B*, 3.

(35) Tully, J. C. In *Dynamics of Molecular Collisions*; Miller, W. H., Ed.; Plenum: New York, 1976; Part B, p 217.

(36) Mead, C. A.; Truhlar, D. G. *J. Chem. Phys.* **1982**, *77*, 6090.

(37) Tully, J. C. *J. Chem. Phys.* **1973**, *59*, 5122.

(38) Numrich, R. W.; Truhlar, D. G. *J. Chem. Phys.* **1975**, *79*, 2745.

(39) Delos, J. B.; Thorson, W. R. *J. Chem. Phys.* **1979**, *70*, 1774.

(40) Baer, M. *Mol. Phys.* **1980**, *40*, 1011.

(41) Sidis, V. *Adv. Chem. Phys.* **1992**, *82*, 187.

(42) Halvick, P.; Truhlar, D. G. *J. Chem. Phys.* **1992**, *96*, 2895.

(43) Ruedenberg, K.; Atchity, G. J. *J. Chem. Phys.* **1993**, *99*, 3799.

(44) Atchity, G. J.; Ruedenberg, K. *Theor. Chem. Acc.* **1997**, *97*, 47.

(45) García, V. M.; Reguero, M.; Caballol, R.; Malrieu, J. P. *Chem. Phys. Lett.* **1997**, *281*, 161.

(46) Topaler, M.; Truhlar, D. G.; Chang, X. Y.; Piecuch, P.; Polanyi, J. C. *J. Chem. Phys.* **1998**, *108*, 5349.

(47) Hack, M. D.; Truhlar, D. G. *J. Chem. Phys.* **1999**, *110*, 4315.

(48) Klüner, T.; Thiel, S.; Staemmler, V. *J. Phys. B* **1999**, *32*, 4931.

(49) Teller, E. *J. Phys. Chem.* **1937**, *41*, 109.

(50) Köppel, H.; Domcke, W.; Cederbaum, L. S. *Adv. Chem. Phys.* **1984**, *57*, 59.

(51) Blais, N. C.; Truhlar, D. G. *J. Chem. Phys.* **1983**, *79*, 1334.

(52) Tully, J. C. *J. Chem. Phys.* **1990**, *93*, 1061.

(53) Kuntz, P. J. *J. Chem. Phys.* **1991**, *95*, 141.

(54) Chapman, S. *Adv. Chem. Phys.* **1992**, *82*, 423.

(55) Meyer, H.-D.; Miller, W. H. *J. Chem. Phys.* **1979**, *70*, 3214.

(56) Micha, D. A. *J. Chem. Phys.* **1983**, *78*, 7138.

(57) Durup, J. *Chem. Phys. Lett.* **1990**, *173*, 537.

(58) García-Vela, A.; Gerber, R. B.; Imre, D. G. *J. Chem. Phys.* **1992**, *97*, 7242.

(59) Gerber, R. B.; Buch, V.; Ratner, M. A. *J. Chem. Phys.* **1982**, *77*, 3022.

(60) Buch, V.; Gerber, R. B.; Ratner, M. A. *Chem. Phys. Lett.* **1983**, *101*, 44.

(61) Alimi, R.; Gerber, R. B.; Hammerich, A. D.; Kosloff, R.; Ratner, M. A. *J. Chem. Phys.* **1990**, *93*, 6484.

(62) Langer, R. E. *Phys. Rev.* **1937**, *51*, 669.

(63) Herman, M. F. *J. Chem. Phys.* **1984**, *81*, 754.

(64) Miller, W. H.; George, T. F. *J. Chem. Phys.* **1972**, *56*, 5637.

(65) Müller, U.; Stock, G. *J. Chem. Phys.* **1997**, *107*, 6230.

(66) Jasper, A. W.; Hack M. D.; Truhlar, D. G., unpublished.

(67) Fang, J.-Y.; Hammes-Schiffer, S. *J. Phys. Chem. A* **1999**, *103*, 9399.

(68) Twain, M. *The Celebrated Jumping Frog of Calaveras County, and Other Sketches*; Paul, J., Ed.; C. H. Webb: New York, 1867.

(69) Herman, M. F. *J. Chem. Phys.* **1999**, *111*, 10427.

(70) R. G. Gordon, J. *Chem. Phys.* **1966**, *44*, 3083.

(71) Blais, N. C.; Truhlar, D. G. *J. Chem. Phys.* **1976**, *65*, 5335.

(72) Truhlar, D. G. *Int. J. Quantum Chem. Symp.* **1976**, *10*, 239.

(73) Truhlar, D. G.; Reid, B. P.; Zurawski, D. E.; Gray, D. E. *J. Phys. Chem.* **1981**, *85*, 786.

(74) Lynch, G. C.; Truhlar, D. G.; Brown, F. B.; Zhao, J. *J. Phys. Chem.* **1995**, *99*, 207.